# **Bi**@hemistry

pubs.acs.org/biochemistry Article

# Steric and Electronic Interactions at Gln154 in ZEITLUPE Induce Reorganization of the LOV Domain Dimer Interface

Ashutosh Pudasaini, Robert Green, Young Hun Song, Abby Blumenfeld, Nischal Karki, Takato Imaizumi, and Brian D. Zoltowski\*



Cite This: Biochemistry 2021, 60, 95-103



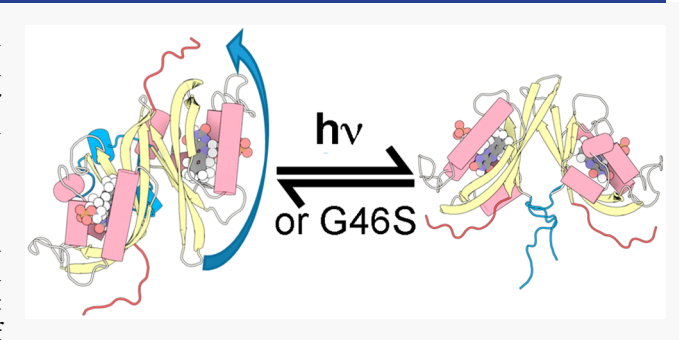
ACCESS

Metrics & More



Supporting Information

ABSTRACT: Plants measure light quality, intensity, and duration to coordinate growth and development with daily and seasonal changes in environmental conditions; however, the molecular details linking photochemistry to signal transduction remain incomplete. Two closely related light, oxygen, or voltage (LOV) domain-containing photoreceptor proteins, ZEITLUPE (ZTL) and FLAVIN-BINDING, KELCH REPEAT, F-BOX 1 (FKF1), divergently regulate the protein stability of circadian clock and photoperiodic flowering components to mediate daily and seasonal development. Using structural approaches, we identified that mutations at the Gly46 position led to global rearrangements of



the ZTL dimer interface in the isolated ZTL-LOV domain. Specifically, G46S and G46A variants induce a 180° rotation about the ZTL-LOV dimer interface that is coupled to ordering of N- and C-terminal signaling elements. These conformational changes hinge upon rotation of a C-terminal Gln residue (Gln154) analogous to that present in light-state structures of ZTL. In contrast to other LOV proteins, a Q154L variant retains light-state interactions with GIGANTEA (GI), thereby indicating N5 protonation is not required for ZTL signaling. The results presented herein confirm a divergent signaling mechanism within ZTL, whereby steric and electronic effects following adduct formation can be sufficient for signal propagation in LOV proteins containing a Gly residue at position 46. Examination of bacterial LOV structures with Gly residues at the equivalent position suggests that mechanisms of signal transduction in LOV proteins may be fluid across the LOV protein family.

Light, oxygen, or voltage (LOV) domain-containing proteins are abundant in nearly all kingdoms of life, where they function as sensory proteins to regulate a diverse array of adaptive responses. Structurally, LOV proteins consist of a central five-stranded β-sheet flanked on one side by four helical elements that cradle a photoactive flavin-based cofactor (FAD, FMN, and riboflavin)<sup>1,3</sup> (Figure 1). Upon photoexcitation, a covalent bond is formed between a conserved cysteine residue and the C4a position of the flavin cofactor (C4a adduct).<sup>4–9</sup> The C4a adduct is reversible in the presence of UVA/violet light or will spontaneously decay in the dark with variable kinetics ranging from seconds to days.<sup>4,6,10</sup> The result is a tunable photochemical sensor that can modulate activity over a wide range of environmental light intensities.<sup>11–13</sup>

Structural and computational studies have linked C4a adduct formation to global conformational changes in protein structure. Existing studies focus on two elements of photoactivation, a change in the hybridization state of the C4a position of the flavin isoalloxazine ring following adduct formation and protonation of the adjacent flavin N5 position. 14–17 Light- and dark-state structures of LOV proteins confirm that N5 protonation causes a flip in the orientation of a conserved Gln residue that alters a hydrogen-bonding

network connected to the  $\beta$ -sheet surface. Alteration in H-bonding interactions dictates either reorganization of the  $\beta$ -sheet surface or alterations in the conformation of N- and C-terminal extensions to the LOV core <sup>15,18,19</sup> (Figure 1). These downstream conformational changes then initiate signal transduction through rearrangement of protein—protein interaction networks or relay photochemical signals to N- or C-terminal signal transduction domains to modulate enzymatic activity in response to changes in blue-light intensity. <sup>1,20–23</sup> In the latter case, the types of signal transduction domains are diverse, leading to LOV domains being viewed as a plug-and-play module that can impart photoactivity to enzymatic function. <sup>1,2,23</sup>

Recent research has indicated that N5 protonation is both necessary and sufficient for photochemical activation. First, studies of LOV variants, which cannot form the C4a adduct

Received: October 8, 2020 Revised: November 27, 2020 Published: December 18, 2020





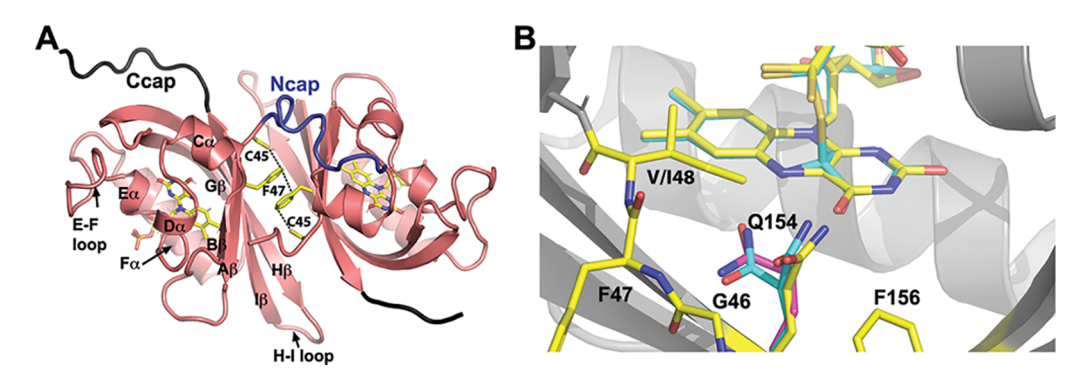


**Figure 1.** Structure and signaling mechanisms of ZTL. (A) Previous ZTL crystal structures consist of an antiparallel dimer mediated by extensive contacts along the  $\beta$ -sheet surface [Protein Data Bank (PDB) entry 5SVG]. A network of sulfur– $\pi$  and  $\pi$ – $\pi$  interactions between Cys45 and Phe47 within the N-cap region stabilize the dimer interface. (B) Crystal structures of ZTL demonstrated an unusual exposed orientation of Gln154 in the dark (yellow; PDB entry 5SVV), compared to a buried orientation in all other LOV structures (magenta, VVD PDB entry 2PD7). Photoactivation in a V48I:G80R variant leads to formation of a C4a adduct (cyan, PDB entry 5SVW) and sp³ hybridization of C4a and protonation of the N5 position. Light-state structures of a V48I:G80R variant indicate that Gln154 may rotate to a buried position following adduct formation.

but retain light-driven photoreduction, are photochemically active and competent for signal transduction. Second,  $Gln \rightarrow Leu$  substitutions that would retain an ability to sense alterations in steric interactions following a hybridization change abrogate signal transduction in most characterized LOV proteins. However, the universality of a Gln-flip mechanism was recently called into question by structures of the plant circadian clock photoreceptor ZEITLUPE (ZTL).

In plants, the ZTL family of photoreceptors consists of ZTL, FLAVIN-BINDING, KELCH REPEAT, F-BOX 1 (FKF1), and LOV KELCH PROTEIN 2 (LKP2). All three are modular LOV proteins, consisting of an N-terminal LOV domain that imparts blue-light regulation of C-terminal F-box and Kelch repeat domains. Absorption of blue light regulates two primary activities: (1) light-driven formation of a ZTL-GIGANTEA (GI) complex, which results in mutual stabilization, and (2) light-driven regulation of E3 ligase activity to allow degradation. Notably, despite conservation of GI complex formation, ZTL and FKF1 differ in the timing of degradation of protein targets, whereby light inhibits ZTL-mediated degradation of circadian clock components, which is enhanced following nightfall. Telephone 27–29 In contrast, light activates the E3 ligase activity of FKF1 allowing enhanced targeted degradation during the day.

Structural studies of the isolated ZTL-LOV domain identified alteration in the canonical mechanism of LOV signal transduction. Namely, structures indicated that the active site Gln residue that is essential for function adopts a heterogeneous conformation under dark-state conditions. Light-state crystal structures revealed that adduct formation led to rotation of Gln154 from an exposed conformation to a buried conformation consistent with all other LOV domain structures (Figure 1B). 11 These structural studies revealed that heterogeneity in the Gln154 conformation was facilitated by the presence of Gly46, which evolutionarily differentiated ZTL from FKF1 and other plant LOV proteins. Unfortunately, these structural studies were based on a ZTL variant containing a V48I substitution that disrupts complete rotation of Gln154, thereby blocking full population of the light state and impeding identification of any global alterations in protein structure. In these regards, the light-state structures are unable to capture the global conformational response attenuating the E3 ligase activity of the effector domains and also unable to identify how signaling mechanisms may differ in ZTL and FKF1 to allow

differential function depending on the time of day. Herein, we employ structural approaches to identify an allosteric mechanism regulating reorganization of the ZTL dimer that is dependent on the residue identity at Gly46. These results confirm an alternative mechanism of signal transduction in ZTL and indicate that LOV allostery may be more fluid across the LOV superfamily.

# ■ MATERIALS AND METHODS

Cloning and Purification. ZTL G46S:G80R and G46A:G80R constructs composed of residues 29-165 were cloned, expressed, and purified with a GST or six-His fusion tag and purified as reported previously. 11 All proteins were purified in 50 mM Tris (pH 7.4), 100 mM NaCl, and 10% glycerol (buffer A). Cells were lysed via sonication at 4 °C. After sonication, the cell debris was separated from the lysate by centrifugation at 18000 rpm and 4 °C for 60 min. Depending on the affinity tag, the proteins were purified using either Ni-NTA or GST affinity columns. The proteins were incubated overnight at 4 °C with 6His-TEV protease to cleave the affinity tags. Cleaved affinity tags and the TEV protease were separated on a Ni-NTA column followed by a final round of purification using fast protein liquid chromatography (FPLC) on a Hiload Superdex 16/60 gel filtration column equilibrated with buffer A.

**Structural Analysis.** ZTL crystals were initially obtained from Hampton Screens (HR2-110 and HR2-112) via the hanging drop method using 1.5  $\mu$ L of a crystallization solution with 1.5  $\mu$ L of a ZTL variant in a concentration range of 5–10 mg/mL. Optimum crystallization conditions were determined for G80R:G46S [0.05 M Tris (pH 8.5) and 2.0 M ammonium sulfate] and G80R:G46A [0.1 M MES (pH 6.0), 1.6 M ammonium sulfate, and 0.01 M cobalt chloride hexahydrate]. Protein for crystallographic studies was purified in buffer A. Crystal trays were set in a dark room illuminated with a red light.

Diffraction data were acquired at the F1 beamline at the Cornell High-Energy Synchrotron Source (CHESS). All data were collected at 100 K. The following cryoprotectants were added: 25% (v/v) ethylene glycol for G80R:G46S and 25% (v/v) ethylene glycol for G80R:G46A. Data reduction and scaling were performed in HKL2000. TL variants were solved using molecular replacement in PHASER that WT ZTL as the search model. Rebuild cycles were performed in COOT,  $^{32}$ 

and the data were refined with PHENIX.<sup>33</sup> Coordinates for G46S:G80R [Protein Data Bank (PDB) entry 6WLP] and G46A:G80R (PDB entry 6WLE) structures can be found in the Protein Data Bank. Data collection and refinement statistics can be found in Table 1.

Table 1. Data Collection and Refinement Statistics (molecular replacement)

	G46S:G80R	G46A:G80R
	Data Collection <sup>a</sup>	
space group	<i>I</i> 213	I213
cell dimensions		
a, b, c (Å)	265.1, 265.1, 265.1	265.8, 265.8, 265.8
$\alpha$ , $\beta$ , $\gamma$ (deg)	90, 90, 90	90, 90, 90
resolution (Å)	3.0 (3.11-3.00)	3.0 (3.11-3.00)
$R_{\text{sym}}$ or $R_{\text{merge}}$	12.8	17.2
$I/\sigma I$	20.9 (2.9)	17.5 (2.6)
completeness (%)	99.9 (99.9)	99.7 (99.9)
redundancy	5.4	6.4
CC <sub>1/2</sub>	0.987 (0.699)	0.994 (0.642)
	Refinement	
resolution (Å)	3.0	3.0
no. of reflections	61740	62237
$R_{\rm work}/R_{\rm free}$	19.3/22.2 (31.8/36.9)	20.3/24.2 (31.0/35.2)
no. of atoms		
protein	7257	7250
ligand/ion	237	229
water	87	87
B-factor		
protein	56.5	52.1
ligand/ion	50.9	45.5
water	42.1	44.6
root-mean-square deviation		
bond lengths (Å)	0.016	0.016
bond angles (deg)	1.60	1.60
		_

<sup>&</sup>lt;sup>a</sup>Data for the highest-resolution shell are shown in parentheses.

SEC-SAXS Sample Preparation and Analysis. All sizeexclusion chromatography-small angle X-ray scattering (SEC-SAXS) samples were purified as outlined in Cloning and Purification with the exception that the final purification buffer contained 50 mM HEPES (pH 8.0), 100 mM NaCl, and 2 mM TCEP, prior to concentration to 20 mg/mL for SAXS studies. SEC-SAXS data were collected at CHESS on beamline G1. Prior to data collection, all samples were centrifuged at 14000 rpm for 20 min. SEC was conducted at 4 °C using a Superdex 200 5/150 column on an AKTA Pure System (GE Healthcare Life Sciences, Marlborough, MA) with a flow rate of 0.15 mL/ min and 0.5 s exposures. The column was equilibrated with 50 mM HEPES (pH 8.0), 100 mM NaCl, and 2 mM TCEP. SAXS data were collected at 9.9099 keV (1.2511 Å) at a rate of  $7.19 \times 10^{11}$  photons/s. The X-ray beam was collimated to 250  $\mu$ m × 250  $\mu$ m diameter and centered on a capillary sample cell with a 1.5 mm path length and 25  $\mu$ m thick quartz glass walls (Charles Supper Co., Natick, MA). The sample cell and full Xray flight path, including beamstop, were kept in vacuo (<1  $\times$ 10<sup>-3</sup> Torr) to eliminate air scatter. The temperature was maintained at 4 °C. Images were collected on a dual Pilatus 100 K-S detector system (Dectris, Baden, Switzerland).

Data processing, image integration, normalization, subtraction, and merging were conducted in BioXTAS RAW

2.0.1.<sup>34</sup> Data were further modeled using software available in the ATSAS software package.<sup>35</sup> Pairwise distribution and Guinier analysis were conducted with GNOM. The *ab initio* molecular envelopes were generated using DAMMIF with *P*1 symmetry. Thirty-five *ab initio* models were constructed, aligned, and averaged using DAMAVER and refined with DAMMIN. The mean normalized spatial discrepancy (NSD) across all models was determined to be 1.118  $\pm$  0.115. One model was found to have an NSD in excess of the mean NSD  $\pm$  2  $\times$  SDV and thus was excluded from the final averaged envelope. The final reported envelope demonstrates a  $\chi^2$  value of 1.191. SAXS data have been deposited in SASBDB (SASDIXS).

**Protein–Protein Interaction Assay.** To overexpress 3xFLAG-6XHis (3F6H) tag-fused ZTL variant proteins, the full-length ZTL, ZTL G46A, ZTL G46S, and ZTL Q154L cDNAs (originally cloned in pENTR/D-TOPO) were introduced into the pB7-HFN binary vector.<sup>36</sup> To analyze protein–protein interactions, the 35S:3F6H-ZTL, 35S:3F6H-ZTL G46A, 35S:3F6H-ZTL G46S, 35S:3F6H-ZTL Q154L, and 35S:HA-GI constructs were infiltrated into 3-week-old Nicotiana benthamiana leaves as described previously.<sup>11</sup>

Co-immunoprecipitation (Co-IP) assays were performed under light-state conditions as described to test proteinprotein interactions between ZTL variants and GI.<sup>37</sup> Briefly, the leaf tissues were harvested and ground in liquid nitrogen. Proteins were extracted from a 0.5 mL volume of the ground tissues using Co-IP buffer [50 mM sodium phosphate (pH 7.4), 150 mM NaCl, 10% glycerol, 5 mM EDTA, 1 mM DTT, 0.1% Triton X-100, 50  $\mu \dot{M}$  MG-132, 2 mM NaVO<sub>4</sub>, 2 mM NaF, and protease inhibitor tablets, EDTA free (Pierce)]. The 3F6H-fused ZTL variants were precipitated (at 4 °C for 10 min under dim light) with the anti-FLAG antibody (Sigma), which was bound to Protein G-coupled magnetic beads (Dynabeads Protein G, Invitrogen). Precipitated proteins were resolved in 8% sodium dodecyl sulfate-polyacrylamide gel electrophoresis gels, and the presence of ZTL variants and HA-GI was detected by Western blot using anti-FLAG (Sigma) and anti-HA (3F10, Roach) antibodies, respectively.

#### RESULTS

Previous studies of the ZTL family identified the LOV domains as obligate dimers formed by extensive contacts along the  $\beta$ -sheet surface. In FKF1, solution scattering experiments indicated that light induces reorganization of an antiparallel FKF1 LOV dimer interface in a manner dependent on the E–F loop; however, structural details regarding the nature of the conformational response are not known. In ZTL, dark- and light-state structures identified two similar antiparallel dimers mediated by contacts across the central  $\beta$ -sheet that differ only by a 2.0 Å translation along the dimer interface. The role of either of these two dimers in signal transduction is currently unknown. In addition, how ZTL and FKF1 may differ at the level of signal transduction is poorly understood.

Previous studies indicated that ZTL has an unusual mechanism of signal transduction that may stem from the evolutionary selection of a Gly residue at position 46. Phylogenetic analysis indicated the residue identity at this position differentiates ZTL (Gly) from other plant LOV proteins, such as FKF1 (Ala or Ser) and phototropins (Asn). Thus, we sought to obtain the crystal structures of G46S and G46A variants of the isolated ZTL LOV domain to examine potential structural and functional differences. In both cases,

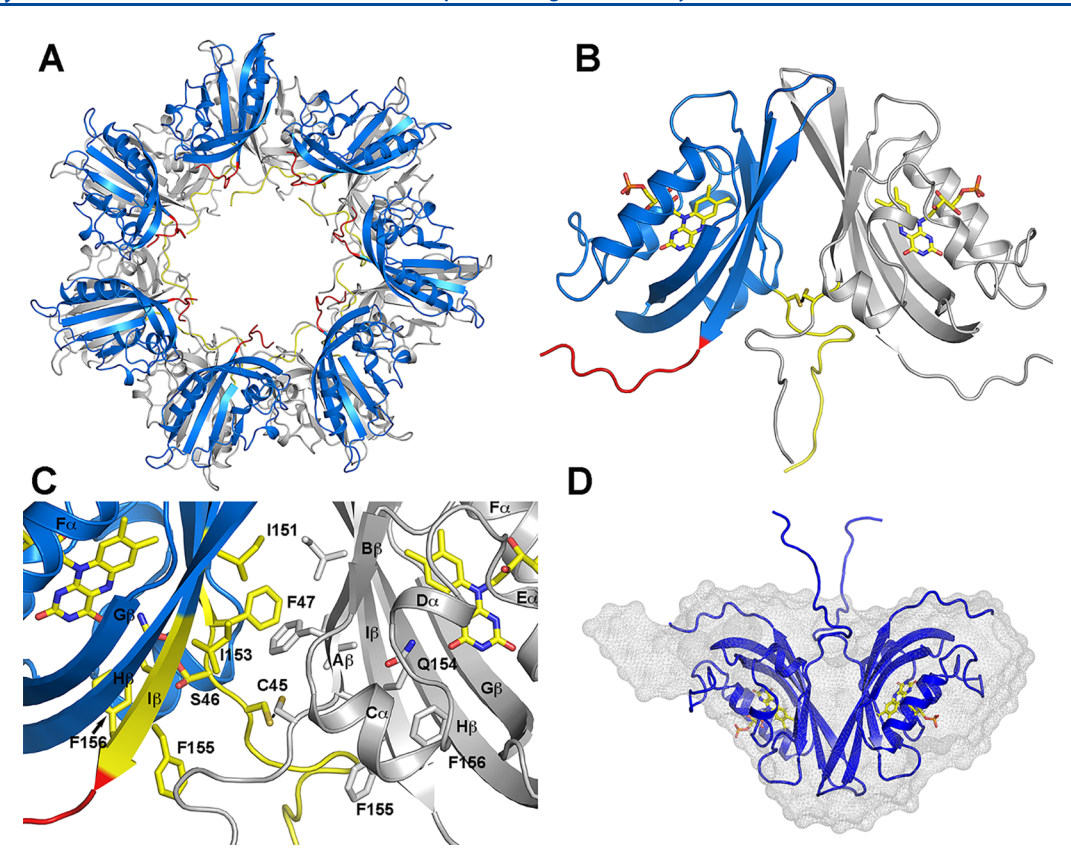


Figure 2. G46A and G46S induce global reorganization of the dimer Interface. (A) G46A:G80R and G46S:G80R crystallize in space group I213 as a 7-fold symmetric ring (blue). The 2-fold screw axis generates a second copy of the 7-fold ring, linked by disulfide-linked dimers in all seven copies. (B) The cross-linked dimer is parallel in orientation and leads to ordering of the N- and C-caps. (C) The parallel dimer is linked through Cys45. Hydrophobic contacts along the β-sheet are similar to those of WT ZTL, involving Phe47, Ile151, and Ile153, but absent the distinguishing sulfur– $\pi$  and  $\pi$ – $\pi$  interactions. (D) SAXS of G46S:G80R variants generates an envelope (gray mesh) consistent with the crystallographic dimer.

proteins had to be studied in the background of a G80R variant that enhances stability but does not affect protein structure. Similar to WT ZTL, the isolated LOV domains of G46A and G46S variants are constitutively dimeric in the dark and light states, suggesting no gross perturbation in structure.<sup>11</sup>

Examination of the dimer interface in the 3.0 Å crystal structures of G46A and G46S reveals distinct structural differences that result from reorientation of Gln154 (Figure 2). As detailed below, reorientation of Gln154 impacts local structure at an N-terminal CGF motif (Cys45-Gly46-Phe47) and a C-terminal QFF motif (Gln154-Phe155-Phe156) that are coupled to global reorientation of the dimer interface. Below, we focus on specific structural differences, beginning at the level of global crystal packing.

Although the core LOV structures of G46A and G46S are highly similar to that of WT ZTL, reorganization of N-terminal and C-terminal elements leads to crystallization in an alternative space group (I213 vs P3121, WT) and grossly alters crystal packing interactions, resulting in dimeric, tetrameric, and heptameric assemblies depending on which molecules are selected in the asymmetric group (Figure 2 and Figure S1). Both G46A and G46S crystallize in a 7-fold symmetric ring involving seven copies of the isolated LOV domain (Figure 2A). N-cap and C-cap elements are well-defined in both structures and orient into a central cavity. In addition, the 2-fold screw axis generates a second copy of the symmetric ring that forms dimeric contacts between individual LOV domains. These dimeric contacts involved the central  $\beta$ -sheet similar to WT ZTL; however, instead of an antiparallel

arrangement observed in WT proteins, Gly46 variants adopt a parallel dimer (Figure 2B,C). Notably, SEC-SAXS confirms G46S:G80R exists as a dimer in solution (MW = 30.8 kDa;  $R_{\rm g}$  = 22.2 Å), and a dimeric assembly is retained on SEC within the detection limits of the method (loading concentration of ~10  $\mu$ M). Moreover, *ab initio* reconstructions of the molecular envelope are consistent with the crystallographic dimer (Figure 2D and Figure S2). Thus, introduction of Gly46 variants leads to a 180° rotation about the  $\beta$ -sheet interface that is coupled to ordering of N-terminal and C-terminal elements.

Although the primary dimeric interface in G46A and G46S still involves the  $\beta$ -scaffold, contacts mediated by the PAS  $\beta$ sheet deviate from those of WT ZTL (Figure 2B,C). Initial inspection of the  $\beta$ -scaffold dimer reveals interactions similar to those of WT ZTL. The  $\beta$ -sheet-directed dimer is stabilized by extensive hydrophobic contacts involving Phe47, Ile151, and Ile153, consistent with WT proteins (Figure 2C). However, the parallel orientation abolishes the sulfur- $\pi$  and  $\pi$ - $\pi$  network present in WT ZTL. Instead, the parallel orientation is facilitated by the formation of disulfide bonds between Cys45 residues (Figure 2B,C). Importantly, treatment of G46A and G46S with TCEP during SEC-SAXS has no effect on dimer formation by SEC (Figure S2). Thus, these disulfides are not required for dimer formation; rather, they likely result from the close interaction of Cys45 that can trap the parallel dimer.

Analysis of the intersection of Gln154 with the CGF and QFF motifs identifies conformational changes facilitating rearrangement of the dimer interface. In both G46A and

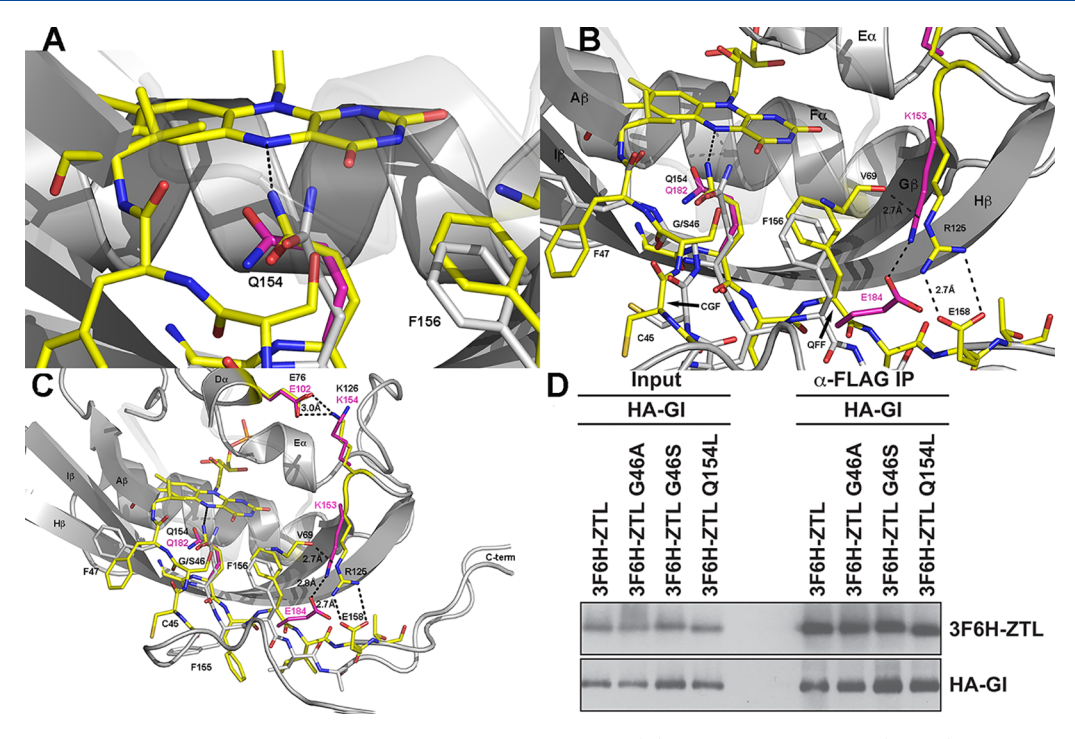


Figure 3. Gln154 reorientation dictates the conformation of the N- and C-termini. (A) Introduction of G46S (yellow) leads to rotation of Gln154 toward the buried conformation (magenta, VVD PDB entry 2PD7) compared to a partially exposed conformation in WT ZTL (gray, PDB entry 5SVG). Rotation of Gln154 is coupled to movement of Phe156 toward the FMN active site. (B and C) Comparative structures of G46S (aqua), WT ZTL (yellow), and VVD (magenta). The altered interactions in G46S are linked to a buried conformation of Q154 that propagates to the N-cap, C-cap, and helical interfaces. These changes are coupled to formation of a salt bridge between Glu158 and Arg125 that are conserved in diverse LOV proteins (VVD colored magenta). These further propagate from the G-H loop (Arg125 and Lys126) to the helical interface through a conserved salt bridge to Glu158. Analogous conformational changes occur in G46A variants (see Figure S1). (D) Confirmation of protein—protein interactions between ZTL variants and GI *in planta* under light-state conditions. ZTL variants were immunoprecipitated with the anti-FLAG antibody, and HA-tagged GI protein was detected with the anti-HA antibody. Similar results were produced twice independently, and the representative image is shown.

G46S, introduction of a side chain leads to a steric clash with exposed conformations of Gln154. These steric contacts push the N-cap away from I $\beta$ , allowing formation of the Cys45 disulfide bond and disruption of the sulfur- $\pi$  interaction network involving Cys45 and Phe47 within the CGF motif (Figure 3). Disruption of the sulfur- $\pi$  interaction network stabilizing the antiparallel dimer leads to a 180° rotation about the WT dimer interface.

In concert with movements at the N-terminal CGF motif, steric interactions between position 46 and the active site Gln154 result in the rotation of Gln154 toward the buried conformation observed in light-state ZTL (Figure 3A-C). Rotation of Gln154 induces movement of Phe156 to partially occupy the region voided by Gln154. These movements draw C-terminal elements closer to the LOV core, partially extending  $\beta$ -sheet-like contacts at the C-terminal end of I $\beta$ . Ordering of the C-terminus results in the formation of a salt bridge between Arg125 within the G-H loop and Glu158 within the C-cap (Figure 3B,C). In addition, the G-H loop makes extensive contacts with the  $C\alpha$  helix. These contacts primarily involve two adjacent, positively charged residues, Arg125 and Lys126. In addition to forming a salt bridge with Glu158, Arg125 forms a H-bond to the carbonyl moiety of Val69 in the  $C\alpha$  helix. The neighboring Lys126 forms an additional salt bridge to Glu76 at the C-terminal end of the D helix. In this manner, Glu158 anchors I $\beta$  to the LOV core, allowing the  $C\alpha$  helix to form a cap directly above the QFF and CGF motifs (Figure 3C). Thus, rotation of Q154 propagates throughout the N-cap and C-cap elements to reorganize the LOV-dimer interface and stabilize interactions between the C-cap and LOV core through new salt bridge interactions. The net result is a more stably folded LOV domain with clear density for both the N-cap and the C-cap.

The results outlined above suggest a divergent signal transduction mechanism in ZTL, whereby the primary signaling element can proceed independent of N5 protonation through steric or electronic changes at the flavin-binding site. If steric or electronic changes are a driving factor for changes in ZTL structure, then Q154L variants may be competent for signal transduction, in contrast to other characterized LOV proteins. To evaluate the necessity of Q154 in ZTL signaling, we examined the effect of Q154L, G46S, and G46A variants on light-activated complex formation with GI in tobacco. Consistent with our hypothesis, all three variants robustly form the ZTL-GI complex following exposure to light (Figure 3D), thereby confirming that Q154L variants are competent for light-state complex formation with GI and that steric and electronic interactions are sufficient for light-induced ZTL-GI complex formation.

#### DISCUSSION

Previous structural studies of the ZTL family of LOV photoreceptors indicated that the signal transduction mechanism of ZTL diverges from those of other LOV proteins, and that photoactivation leads to rearrangement of a dimer interface. However, the precise nature of the global

reorganization remained elusive due to either the lack of atomic-resolution crystal structures (FKF1) or the presence of mutations that block global reorganization of the protein (ZTL). Herein, we have identified a protein variant that traps a light-state-like orientation of the active site Gln residue in crystal structures. The resulting structures allow a snapshot of global reorganization following rotation of Gln154 from the exposed (dark) to buried (light-like) conformation. The new crystal structures shed light on ZTL function and signal transduction within the LOV superfamily.

Comparison of the ZTL crystal structures identifies a conserved topology of signal transduction in LOV proteins. First, photoactivation results in two primary signal-inducing events, protonation of the N5 position and an sp<sup>2</sup> to sp change in hybridization at the C4a position. 6,8,15 Second, studies of the LOV protein VVD and an engineered LOV histidine kinase, YF1, confirmed that N5 protonation was both necessary and sufficient for photoactivation. 16 Here, we show that ZTL adopts an alternative signaling mechanism, whereby an H-bonding residue at the Gln154 position is not necessary, and light-state functionality is retained in a Q154L variant. An altered mechanism of signal transduction is consistent with sequence analysis of ZTL family proteins, where LKP2 proteins and homologues in Brassica rapa all contain Leu residues at the position equivalent to Gln154. 11 In all cases, these proteins retain a Gly residue at the position equivalent to Gly46. How these proteins transduce a signal, and if a similar signaling pathway is retained in other LOV proteins, are open questions. On the basis of our structural studies of G46A and G46S variants in ZTL, and prior studies in other LOV systems, we propose a possible signaling mechanism and extend our model to other LOV systems.

Our proposed signaling mechanism results from three elements linking flavin electronics and steric constraints to downstream signal transduction. (1) The presence of Gly46 permits alternative conformations of Gln154. These include an exposed conformation with strong H-bonds to the flavin O4 position. (2) In WT ZTL, adduct formation results in alteration of the flavin electronic structure, thereby disfavoring strong H-bonding interactions at the flavin O4 position and leading to movement of the active site Gln. We note that a similar mechanism was predicted in early computational studies of Avena sativa phototropin LOV2, where strong Hbonds to O4 trapped Gln513 (AsLOV2 numbering) in an exposed conformation that was relieved following adduct formation.<sup>39</sup> (3) In ZTL Q154L and LKP2-like proteins containing a Leu residue at position 154, an alternative mechanism linking flavin electronics and steric constraints can persist. Specifically, we propose that changes in the flavin electronic structure dictate movement of Phe residues coupled to the active site flavin. Movement of these Phe residues impinges on steric interactions at the Q154 locus. Specifically, in the case of ZTL, the conserved Phe156 moves toward the flavin active site, necessitating movement of either Gln154 or Leu154 residues occupying an exposed-like conformation. Notably, a Phe residue at this position is unique to members of the ZTL family and is highly conserved (Figure S3C). As outlined below, our proposed mechanism is consistent with recent structural and computational studies of bacterial LOV domain-containing photoreceptors.

First, central to our proposed mechanism is the ability of Gly residues at position 46 to permit alternative exposed conformations of the active site Gln. Three other LOV

proteins that contain a Gly residue at the position equivalent to Gly46 have been structurally characterized (Figure 4 and

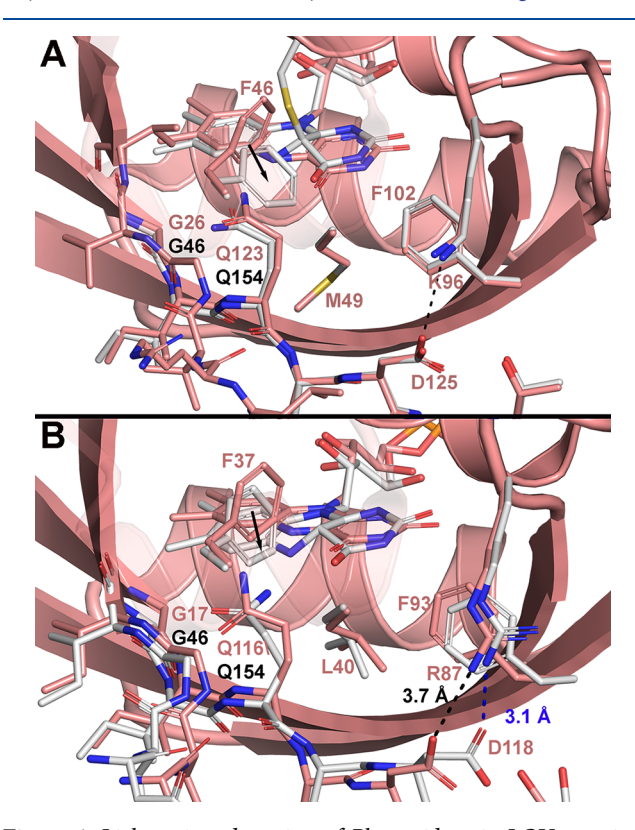


Figure 4. Light-activated motion of Phe residues in LOV proteins. (A) YtvA and (B) PpLOV contain Gly residues at position 46 (ZTL numbering, black), contain unusual orientations of the active site Gln154 (ZTL numbering, black), and couple salt bridge formation and Gln ordering to movement of conserved Phe residues. (A) Phe46 undergoes a light-driven conformational change (black arrow) in YtvA (gray, light YtvA, PDB entry 2PR6, and salmon, dark YtvA, PDB entry 2PR5). Computational studies demonstrate alternative conformations of Q123 that is coupled to Phe46 and salt bridge formation (K96–D125). (B) Phe37 undergoes a light-driven conformational change in PpLOV (black arrow). Dark-state PpLOV (salmon) contains an unusual conformation of Q116 that becomes ordered upon light activation (gray). Light activation induces formation of a salt bridge between Arg87 and Asp118. Comparisons of YtvA, PpLOV, CaLOV, and ZTL can be found in Figure S3.

Figure S3). These include YtvA, <sup>40</sup> a short LOV protein from *Pseudomonas putida* (PpLOV), <sup>41,42</sup> and a LOV domain from *Chloroflexus aggregans* (CaLOV). <sup>43</sup> Structural studies of dark-state CaLOV demonstrate occupancy of both buried and exposed conformations of the active site Gln identical to ZTL (Figure S3). <sup>43</sup> In addition, recent computational studies of YtvA indicate rapid interconversion of the active site Gln (Gln123) between exposed and buried conformations in the dark, which becomes ordered following adduct formation. <sup>40</sup> Similarly, dark-state structures of PpLOV (Figure 3B and Figure S3) demonstrate an unusual exposed-like conformation of the active site Gln (Gln116), which becomes ordered in a buried conformation upon light treatment. <sup>41,42</sup>

Second, close examination of light- and dark-state structures of YtvA and PpLOV indicates that ordering of the active site Gln following adduct formation is tightly coupled to light-dependent conformational changes in conserved Phe residues, 40-42 and salt bridge formation in residues positioned

similar to Arg125-Glu158 (Figure 4 and Figure S3). In all cases, movement of the Phe residues would sterically clash with an exposed Gln conformation. Notably, in computational studies of YtvA, F46A variants disrupted the Gln123 landscape, consistent with a specific role of Phe residues in dictating Gln conformational changes mediating LOV signal transduction. 40 In addition, in the case of YtvA and PpLOV, Gln movement following adduct formation is coupled to salt bridge formation at sites similar to the ZTL Arg125-Glu158 salt bridge (Figure 4). Notably, analogous light-dependent salt bridge formation has been observed in computational studies of Neurospora crassa VVD, 44 indicating such a mechanism may be widespread in LOV proteins. Such a mechanism is linked to the residue identity at Gly46, which permits exposed-like conformations of the active site Gln, and light-dependent movement of conserved Phe residues that sterically constrain residues at the position equivalent to ZTL Gln154. These results suggest that an analogous mechanism independent of N5-Gln H-bonds may function in YtvA, PpLOV, and/or CaLOV. Indeed, in YtvA, although we are unaware of Q123L variants being studied, a Q123A variant retains 50% of WT function in YtvA, 45 indicating that an altered mechanism of signal transduction can persist in YtvA and likely other LOV proteins.

Overall, our proposed mechanism links signaling motifs within  $A\beta$  (CGF motif) and  $I\beta$  (QFF motif) to enable an altered Gln154 landscape and signaling response, where changes to the flavin electronic structure result in concerted movement of Gln154 and Phe156. These movements result in ordering of the C-termini and induction of a stabilizing salt bridge. In concert with C-terminal conformational changes, the  $A\beta$  strand moves away from the LOV core, destabilizing the antiparallel dimer interface and leading to a 180° rotation about the central  $\beta$ -scaffold. In these regards, the initial driving force of an allosteric response (hybridization, H-bonds, and electronic structure) may diverge in LOV proteins; however, they conserve signaling elements that enable order—disorder transitions at the N- and C-termini that hinge upon residue selection at a key allosteric signaling site (Gly46).

Effects on ZTL Signal Transduction. ZTL crystal structures confirm that the alteration in the ZTL signaling mechanism stems from the unusual evolutionary selection of Gly46. The equivalent residue is an Ala/Ser in fungal LOV and in plant FKF1 proteins or an Asn in plant phototropins. 11 In these cases, the residue occupying that position is involved in alterations in H-bonding interactions following the Gln-flip mechanism, enabling adduct formation to signal to the N- and C-termini of LOV proteins. 8,11,15,17 In ZTL, the Gly residue is unable to respond to H-bond changes; rather, the lack of a side chain permits alternative conformations of Gln154, enabling an alternative electronics-sensing mechanism to proceed. Introduction of an Ala/Ser residue in ZTL introduces steric constraints on Gln154, which invokes a light-state-like rearrangement of the dimer interface by promoting concerted movements of Gln154, the N-terminal CGF motif, and the Cterminal QFF motif. These observations led us to postulate about the signaling differences between ZTL and FKF1 proteins in plant photobiology.

The biological activity of ZTL hinges upon two fundamental light-regulated events. First, blue light induces a conformational change within the N-terminal LOV domain that enhances LOV-mediated protein—protein interactions with GI.<sup>29,46</sup> The resulting complex mutually stabilizes both proteins, resulting in the accumulation of ZTL and GI during

the day. In conjunction with ZTL-GI complex formation, light inhibits the E3 ligase activity of ZTL, leading to decreased rates of degradation of ZTL targets PRR5 and TOC1. 11,27,28,47–49 Throughout the night, decay of the C4a adduct activates ZTL-mediated degradation activity, allowing turnover of PRR5 and TOC1 in a manner that is dependent on the time of day. How ZTL structural rearrangements, particularly in relation to the role of LOV-mediated dimers, impact degradation activity is currently unknown. Here, we observe that introduction of G46S resulted in two consequences: (1) stabilization of N- and C-terminal elements consistent with increased stability of ZTL in the light state and (2) the ZTL LOV domain undergoing a 180° rotation about the LOV dimer interface to favor a parallel orientation. We propose that rearrangement of the LOV dimer interface leads to a decrease in E3 ligase activity for light-state ZTL.

#### ASSOCIATED CONTENT

# **Supporting Information**

The Supporting Information is available free of charge at https://pubs.acs.org/doi/10.1021/acs.biochem.0c00819.

Alternative assemblies in the crystal lattice and Gln154 orientations (Figure S1), SEC-SAXS data and analysis (Figure S2), and comparison of LOV structures containing a Gly at position 46 (Figure S3) (PDF)

#### **Accession Codes**

ZTL, Q94BT6 (Uniprot).

# AUTHOR INFORMATION

# **Corresponding Author**

Brian D. Zoltowski — Department of Chemistry, Southern Methodist University, Dallas, Texas 75275, United States; Center for Drug Discovery, Design and Delivery, Southern Methodist University, Dallas, Texas 75275, United States; orcid.org/0000-0001-6749-0743; Phone: 214-768-2640; Email: bzoltowski@smu.edu; Fax: 214-768-4089

#### **Authors**

Ashutosh Pudasaini — Department of Chemistry, Southern Methodist University, Dallas, Texas 75275, United States; Center for Drug Discovery, Design and Delivery, Southern Methodist University, Dallas, Texas 75275, United States

Robert Green – Department of Chemistry, Southern Methodist University, Dallas, Texas 75275, United States; Center for Drug Discovery, Design and Delivery, Southern Methodist University, Dallas, Texas 75275, United States

**Young Hun Song** — Department of Agricultural Biotechnology, Seoul National University, Seoul 08826, Korea

Abby Blumenfeld – Department of Chemistry, Southern Methodist University, Dallas, Texas 75275, United States; Center for Drug Discovery, Design and Delivery, Southern Methodist University, Dallas, Texas 75275, United States

Nischal Karki — Department of Chemistry, Southern Methodist University, Dallas, Texas 75275, United States; Center for Drug Discovery, Design and Delivery, Southern Methodist University, Dallas, Texas 75275, United States

Takato Imaizumi — Department of Biology, University of Washington, Seattle, Washington 98195-1800, United States

Complete contact information is available at: https://pubs.acs.org/10.1021/acs.biochem.0c00819

#### **Author Contributions**

A.P. and R.G. contributed equally to this work. Protein expression, purification, and structural characterization of ZTL G46S and G46A constructs were conducted by A.P., R.G., and B.D.Z. A.B. and N.K. conducted SAXS data analysis. Protein interaction studies in plant tissues were conducted by Y.H.S. and T.I. All contributed to the writing of the manuscript.

#### **Funding**

This work was funded by the National Institutes of Health (Grants 2R15GM109282 to B.D.Z. and R01GM079712 to T.I.) and by the Nuclear R&D Program of the Ministry of Science and ICT (MSIT), Republic of Korea (Y.H.S.). Y.H.S. and T.I. are also supported by the Next-Generation BioGreen 21 Program (SSAC, PJ013386, Rural Development Administration, Republic of Korea).

#### **Notes**

The authors declare no competing financial interest.

# REFERENCES

- (1) Crosson, S., Rajagopal, S., and Moffat, K. (2003) The LOV domain family: photoresponsive signaling modules coupled to diverse output domains. *Biochemistry* 42, 2-10.
- (2) Pudasaini, A., El-Arab, K. K., and Zoltowski, B. D. (2015) LOV-based optogenetic devices: light-driven modules to impart photoregulated control of cellular signaling. *Front. Mol. Biosci.* 2, 18.
- (3) Zoltowski, B. D., and Gardner, K. H. (2011) Tripping the Light Fantastic: Blue-Light Photoreceptors as Examples of Environmentally Modulated Protein-Protein Interactions. *Biochemistry* 50, 4–16.
- (4) Alexandre, M. T. A., Arents, J. C., van Grondelle, R., Hellingwerf, K. J., and Kennis, J. T. M. (2007) A Base-Catalyzed Mechanism for Dark State Recovery in the *Avena Sativa* Phototropin-1 LOV2 Domain. *Biochemistry* 46, 3129–3137.
- (5) Kennis, J. T., Crosson, S., Gauden, M., van Stokkum, I. H., Moffat, K., and van Grondelle, R. (2003) Primary reactions of the LOV2 domain of phototropin, a plant blue-light photoreceptor. *Biochemistry* 42, 3385–3392.
- (6) Kennis, J. T., van Stokkum, I. H., Crosson, S., Gauden, M., Moffat, K., and van Grondelle, R. (2004) The LOV2 domain of phototropin: a reversible photochromic switch. *J. Am. Chem. Soc.* 126, 4512–4513.
- (7) Kottke, T., Hegemann, P., Dick, B., and Heberle, J. (2006) The Photochemistry of the Light-, Oxygen-, and Voltage- Sensitive Domains in the Algal Blue Light Receptor Phot. *Biopolymers* 82, 373–378.
- (8) Crosson, S., and Moffat, K. (2002) Phototexcited structure of a plant photoreceptor domain reveals a light-driven molecular switch. *Plant Cell* 14, 1067–1075.
- (9) Salomon, M., Christie, J. M., Knieb, E., Lempert, U., and Briggs, W. R. (2000) Photochemical and mutational analysis of the FMN-binding domains of the plant blue light receptor, phototropin. *Biochemistry* 39, 9401–9410.
- (10) Zoltowski, B. D., Vaccaro, B., and Crane, B. R. (2009) Mechanism-based tuning of a LOV domain photoreceptor. *Nat. Chem. Biol.* 5, 827–834.
- (11) Pudasaini, A., Shim, J. S., Song, Y. H., Shi, H., Kiba, T., Somers, D. E., Imaizumi, T., and Zoltowski, B. D. (2017) Kinetics of the LOV domain of ZEITLUPE determine its circadian function in Arabidopsis. *eLife* 6, No. e21646.
- (12) Pudasaini, A., and Zoltowski, B. D. (2013) Zeitlupe senses blue-light fluence to mediate circadian timing in Arabidopsis thaliana. *Biochemistry* 52, 7150–7158.
- (13) Bannister, S., Bohm, E., Zinn, T., Hellweg, T., and Kottke, T. (2019) Arguments for an additional long-lived intermediate in the photocycle of the full-length aureochrome 1c receptor: A time-resolved small-angle X-ray scattering study. *Struct. Dyn. 6*, 034701.
- (14) Tang, Y. F., Cao, Z., Livoti, E., Krauss, U., Jaeger, K. E., Gartner, W., and Losi, A. (2010) Interdomain signalling in the blue-

- light sensing and GTP-binding protein YtvA: A mutagenesis study uncovering the importance of specific protein sites. *Photochemical & Photobiological Sciences 9*, 47–56.
- (15) Vaidya, A. T., Chen, C. H., Dunlap, J. C., Loros, J. J., and Crane, B. R. (2011) Structure of a light-activated LOV protein dimer that regulates transcription. *Sci. Signaling* 4, No. ra50.
- (16) Yee, E. F., Diensthuber, R. P., Vaidya, A. T., Borbat, P. P., Engelhard, C., Freed, J. H., Bittl, R., Moglich, A., and Crane, B. R. (2015) Signal transduction in light-oxygen-voltage receptors lacking the adduct-forming cysteine residue. *Nat. Commun.* 6, 10079.
- (17) Zoltowski, B. D., Schwerdtfeger, C., Widom, J., Loros, J. J., Bilwes, A. M., Dunlap, J. C., and Crane, B. R. (2007) Conformational Switching in the Fungal Light Sensor Vivid. *Science* 316, 1054–1057.
- (18) Bocola, M., Schwaneberg, U., Jaeger, K. E., and Krauss, U. (2015) Light-induced structural changes in a short light, oxygen, voltage (LOV) protein revealed by molecular dynamics simulations—implications for the understanding of LOV photoactivation. *Front. Mol. Biosci.* 2, 55.
- (19) Nozaki, D., Iwata, T., Ishikawa, T., Todo, T., Tokutomi, S., and Kandori, H. (2004) Role of Gln1029 in the Photoactivation Processes of the LOV2 Domain in Adiantum Phytochrome3. *Biochemistry* 43, 8373–8379.
- (20) Alexandre, M. T., van Grondelle, R., Hellingwerf, K. J., Robert, B., and Kennis, J. T. (2008) Perturbation of the ground-state electronic structure of FMN by the conserved cysteine in phototropin LOV2 domains. *Phys. Chem. Chem. Phys.* 10, 6693–6702.
- (21) Christie, J. M. (2007) Phototropin blue-light receptors. Annu. Rev. Plant Biol. 58, 21–45.
- (22) Moglich, A., and Moffat, K. (2007) Structural basis for light-dependent signaling in the dimeric LOV domain of the photosensor YtvA. *J. Mol. Biol.* 373, 112–126.
- (23) Losi, A., Gardner, K. H., and Moglich, A. (2018) Blue-Light Receptors for Optogenetics. *Chem. Rev.* 118, 10659–10709.
- (24) Nash, A. I., Ko, W. H., Harper, S. M., and Gardner, K. H. (2008) A conserved glutamine plays a central role in LOV domain signal transmission and its duration. *Biochemistry* 47, 13842–13849.
- (25) Somers, D. E., Kim, W. Y., and Geng, R. S. (2004) The F-box protein ZEITLUPE confers dosage-dependent control on the circadian clock, photomorphogenesis, and flowering time. *Plant Cell* 16, 769–782.
- (26) Zoltowski, B. D., and Imaizumi, T. (2014) Structure and Function of the ZTL/FKF1/LKP2 Group Proteins in Arabidopsis. *Enzymes* 35, 213–239.
- (27) Baudry, A., Ito, S., Song, Y. H., Strait, A. A., Kiba, T., Lu, S., Henriques, R., Pruneda-Paz, J. L., Chua, N. H., Tobin, E. M., Kay, S. A., and Imaizumi, T. (2010) F-Box Proteins FKF1 and LKP2 Act in Concert with ZEITLUPE to Control Arabidopsis Clock Progression. *Plant Cell* 22, 606–622.
- (28) Ito, S., Song, Y. H., and Imaizumi, T. (2012) LOV domain-containing F-box proteins: light-dependent protein degradation modules in Arabidopsis. *Mol. Plant* 5, 573–582.
- (29) Kim, W. Y., Fujiwara, S., Suh, S. S., Kim, J., Kim, Y., Han, L. Q., David, K., Putterill, J., Nam, H. G., and Somers, D. E. (2007) ZEITLUPE is a circadian photoreceptor stabilized by GIGANTEA in blue light. *Nature* 449, 356–360.
- (30) Otwinowski, A., and Minor, W. (1997) Processing of X-ray diffraction data in oscillation mode. *Methods Enzymol.* 276, 307–325.
- (31) Mccoy, A. J., Grosse-Kunstleve, R. W., Adams, P. D., Winn, M. D., Storoni, L. C., and Read, R. J. (2007) Phaser crystallographic software. *J. Appl. Crystallogr.* 40, 658–674.
- (32) Emsley, P., and Cowtan, K. (2004) Coot: model-building tools for molecular graphics. *Acta Crystallogr., Sect. D: Biol. Crystallogr.* 60, 2126–2132.
- (33) Adams, P. D., Afonine, P. V., Bunkoczi, G., Chen, V. B., Davis, I. W., Echols, N., Headd, J. J., Hung, L. W., Kapral, G. J., Grosse-Kunstleve, R. W., McCoy, A. J., Moriarty, N. W., Oeffner, R., Read, R. J., Richardson, D. C., Richardson, J. S., Terwilliger, T. C., and Zwart, P. H. (2010) PHENIX: a comprehensive Python-based system for

- macromolecular structure solution. Acta Crystallogr., Sect. D: Biol. Crystallogr. 66, 213–221.
- (34) Hopkins, J. B., Gillilan, R. E., and Skou, S. (2017) BioXTAS RAW: improvements to a free open-source program for small-angle X-ray scattering data reduction and analysis. *J. Appl. Crystallogr.* 50, 1545–1553.
- (35) Petoukhov, M. V., Franke, D., Shkumatov, A. V., Tria, G., Kikhney, A. G., Gajda, M., Gorba, C., Mertens, H. D., Konarev, P. V., and Svergun, D. I. (2012) New developments in the ATSAS program package for small-angle scattering data analysis. *J. Appl. Crystallogr.* 45, 342–350.
- (36) Lee, C. M., Adamchek, C., Feke, A., Nusinow, D. A., and Gendron, J. M. (2017) Mapping Protein-Protein Interactions Using Affinity Purification and Mass Spectrometry. *Methods Mol. Biol.* 1610, 231–249.
- (37) Song, Y. H., Smith, R. W., To, B. J., Millar, A. J., and Imaizumi, T. (2012) FKF1 conveys timing information for CONSTANS stabilization in photoperiodic flowering. *Science* 336, 1045–1049.
- (38) Nakasako, M., Matsuoka, D., Zikihara, K., and Tokutomi, S. (2005) Quaternary structure of LOV-domain containing polypeptide of Arabidopsis FKF1 protein. *FEBS Lett.* 579, 1067–1071.
- (39) Freddolino, P. L., Gardner, K. H., and Schulten, K. (2013) Signaling mechanisms of LOV domains: new insights from molecular dynamics studies. *Photochemical & photobiological sciences: Official journal of the European Photochemistry Association and the European Society for Photobiology* 12, 1158–1170.
- (40) Polverini, E., Schackert, F. K., and Losi, A. (2020) Interplay among the "flipping" glutamine, a conserved phenylalanine, water and hydrogen bonds within a blue-light sensing LOV domain. *Photochemical & photobiological sciences: Official journal of the European Photochemistry Association and the European Society for Photobiology* 19, 892–904.
- (41) Circolone, F., Granzin, J., Jentzsch, K., Drepper, T., Jaeger, K. E., Willbold, D., Krauss, U., and Batra-Safferling, R. (2012) Structural basis for the slow dark recovery of a full-length LOV protein from Pseudomonas putida. *J. Mol. Biol.* 417, 362–374.
- (42) Rollen, K., Granzin, J., Panwalkar, V., Arinkin, V., Rani, R., Hartmann, R., Krauss, U., Jaeger, K. E., Willbold, D., and Batra-Safferling, R. (2016) Signaling States of a Short Blue-Light Photoreceptor Protein PpSB1-LOV Revealed from Crystal Structures and Solution NMR Spectroscopy. *J. Mol. Biol.* 428, 3721–3736.
- (43) Nazarenko, V. V., Remeeva, A., Yudenko, A., Kovalev, K., Dubenko, A., Goncharov, I. M., Kuzmichev, P., Rogachev, A. V., Buslaev, P., Borshchevskiy, V., Mishin, A., Dhoke, G. V., Schwaneberg, U., Davari, M. D., Jaeger, K. E., Krauss, U., Gordeliy, V., and Gushchin, I. (2019) A thermostable flavin-based fluorescent protein from Chloroflexus aggregans: a framework for ultra-high resolution structural studies. *Photochemical & photobiological sciences: Official journal of the European Photochemistry Association and the European Society for Photobiology* 18, 1793–1805.
- (44) Zhou, H., Zoltowski, B. D., and Tao, P. (2017) Revealing Hidden Conformational Space of LOV Protein VIVID Through Rigid Residue Scan Simulations. *Sci. Rep.* 7, 46626.
- (45) Avila-Perez, M., Vreede, J., Tang, Y., Bende, O., Losi, A., Gartner, W., and Hellingwerf, K. (2009) In vivo mutational analysis of YtvA from Bacillus subtilis: mechanism of light activation of the general stress response. *J. Biol. Chem.* 284, 24958–24964.
- (46) Cha, J. Y., Kim, J., Kim, T. S., Zeng, Q., Wang, L., Lee, S. Y., Kim, W. Y., and Somers, D. E. (2017) GIGANTEA is a co-chaperone which facilitates maturation of ZEITLUPE in the Arabidopsis circadian clock. *Nat. Commun.* 8, 3.
- (47) Harmer, S. L. (2009) The Circadian System in Higher Plants. *Annu. Rev. Plant Biol.* 60, 357–377.
- (48) Lee, C. M., Feke, A., Li, M. W., Adamchek, C., Webb, K., Pruneda-Paz, J., Bennett, E. J., Kay, S. A., and Gendron, J. M. (2018) Decoys Untangle Complicated Redundancy and Reveal Targets of Circadian Clock F-Box Proteins. *Plant Physiol.* 177, 1170–1186.

(49) Mas, P., Kim, W. Y., Somers, D. E., and Kay, S. A. (2003) Targeted degradation of TOC1 by ZTL modulates circadian function in Arabidopsis thaliana. *Nature* 426, 567–570.